Carbohydrate Polymers 90 (2012) 592–601

Contents lists available at SciVerse ScienceDirect

Carbohydrate Polymers

journal homepage: www.elsevier.com/locate/carbpol

# Electrospun PCL/phlorotannin nanofibres for tissue engineering: Physical properties and cellular activities

Minseong Kim[a,b], GeunHyung Kim[a,*]

[a] Bio/Nanofluidics Lab, Department of Mechanical Engineering, Chosun University, Gwangju 501-759, South Korea
[b] School of Medicine, Chosun University, Gwangju 501-759, South Korea

ARTICLE INFO

*Article history:*
Received 13 January 2012
Received in revised form 14 April 2012
Accepted 22 May 2012
Available online 30 May 2012

*Keywords:*
Phlorotannin
Polycaprolactone
Biocomposite
Bone
Tissue regeneration

ABSTRACT

Micro/nanofibrous substrates have been widely used for tissue regeneration because of their similarities to extracellular matrix components and their high surface area, which facilitates attachment and proliferation of cells. Phlorotannin, the main component of the brown alga *Ecklonia cava*, contains various growth factors that promote the regeneration of various tissues, including bone, by stimulating alkaline phosphatase (ALP) activity and inducing calcium deposition. Despite the benefits of phlorotannin in tissue regeneration, the activity of phlorotannin as a component of micro/nanofibres of various compositions has not yet been investigated. Here, we fabricated electrospun polycaprolactone (PCL)/phlorotannin micro/nanofibres containing different phlorotannin concentrations (1, 3, and 5 wt%) and determined their physical properties, including water contact angle, water absorption, and mechanical properties. Owing to their hydrophilicity and water absorption ability, phlorotannin-containing fibrous mats exhibited outstanding wettability compared with pure PCL fibrous mats. The biocompatibility of the mats was examined in vitro using osteoblast-like cells (MG63). Cell viability, ALP activity, and calcium deposition were assessed. The cells distributed more widely and proliferated to a greater degree on PCL/phlorotannin mats compared with pure PCL mats. In addition, cell viability (at 5 wt% phlorotannin), total protein content, ALP activity, and calcium deposition were higher with PCL/phlorotannin mats than with pure PCL mats. These results suggest that electrospun PCL/phlorotannin is a promising bioactive material for enhancing bone tissue growth.



## 1. Introduction

Tissue engineering comprises inter-disciplinary research efforts to regenerate damaged tissues and organs (Hirano & Mooney, 2004; Khademhosseini, Langer, Borenstein, & Vacanti, 2006). Successful tissue regeneration relies on biocompatible scaffolds designed to provide sites for cell attachment and proliferation, transport paths for nutrients and waste, and mechanical support for enduring environmental stress (Hollister, 2005; Ma, 2004). According to several studies, nano-topographical shapes (pores, ridges, groves, fibres, nodes, and combinations of these shapes) can influence attachment, proliferation, morphology, endocytotic activity, and gene expression of various cell types (Kumbar, James, Nukavarapu, & Laurencin, 2008).

Electrospinning is a common method to fabricate micro/nanofibres. In the process, polymer solution can be ejected from a syringe and formed into a suspended droplet at the tip of the nozzle. When a high electric field is applied to the nozzle tip and the electrostatic force acting on the suspended polymeric solution overcomes the surface tension of the solution, micro/nanofibres can be generated from the apex of the Taylor cone (Doshi & Reneker, 1995; Formhals, 1934; Luo, Stride, Stoyanov, Pelan, & Edirisinghe, 2011; Taylor, 1964). Fabricated micro/nanofibres have various applications, including as chemical sensors, electronic materials, membrane filtration, protective cloth, composite materials, and biomedical scaffolds (Bergshoef & Vancso, 1999; Fong, Chun, & Reneker, 1999; Greiner & Wendorff, 2007; Hong & Kim, 2010; Huang, Zhang, Kotaki, & Ramakrishna, 2003; Kim & Kim, 2006).

Algae contain various polysaccharides, minerals, and vitamins with biological activities such as antimicrobial, antioxidant, antiviral, and antitumour activities. Algae components have also been shown to control or prevent various conditions, including myocardial infarction, hypertension, angina pectoris, and stroke (Chen & Chou, 2002; Frlich & Riederer, 1995; Nagayama, Iwamura, Shibata, Hirayama, & Nakamura, 2002; Okai et al., 1998). *Ecklonia cava* (EC) is a brown seaweed found off the coast of Jeju Island, South Korea. EC contains a number of biologically active materials, and its applications are expanding (Cho & Choi, 2010; Jimenez-Escring & Goni Cambrodon, 1999). In particular, phlorotannin, one of the

* Corresponding author. Tel.: +82 62 230 7180; fax: +82 62 236 1534.
*E-mail address:* gkim@chosun.ac.kr (G. Kim).

0144-8617/$ – see front matter © 2012 Elsevier Ltd. All rights reserved.
http://dx.doi.org/10.1016/j.carbpol.2012.05.082

main components of EC, is a polyphenol compound composed of phloroglucinol as a basic unit. The abilities of phlorotannin to interfere with thrombosis, protect the cardiovascular system, and combat viruses have been investigated (Ahn et al., 2004; Kang et al., 2003). In terms of tissue engineering, phlorotannin at non-cytotoxic concentrations has been demonstrated to induce osteoblast proliferation by enhancing collagen, alkaline phosphatase (ALP) activity, and calcium deposition (Ryu, Li, Qian, Kim, & Kim, 2009).

For the biological activities of phlorotannin to benefit tissue engineering, phlorotannin must be formed into shapes that facilitate cell attachment and proliferation. To this end, we developed micro/nanofibrous structures consisting of polycaprolactone (PCL) and phlorotannin (Ph), using different phlorotannin concentrations (1, 3, and 5 wt%) with a constant weight fraction of PCL. The biocompatibility of mats formed from these micro/nanofibres was examined in vitro using osteoblast-like cells (MG63). Cell viability, ALP activity, and calcium deposition of MG63 cells on micro/nanofibrous mats were analysed. In addition, physical properties of the mats, including water contact angle, water absorption, and mechanical properties, were determined.

## 2. Materials and experimental methods

### 2.1. Materials

A PCL solution was prepared by dissolving 2.4 g of PCL ($M_w$ = 80,000; St. Louis, MO, USA) in 30 g of a solvent mixture of 80 wt% methylene chloride (Junsei) and 20 wt% dimethylformamide (Junsei). Different amounts of powdered phlorotannin were then added; greater than 5 wt% phlorotannin resulted in inadequate electrospinning of the PCL/phlorotannin solution, such that the obtained fibres exhibited string-bead shapes. Therefore, we used a maximum of 5 wt% phlorotannin.

### 2.2. Preparation of phlorotannin from EC extract

The brown seaweed *E. cava* was collected from the coast of Jeju Island between October 2008 and March 2009. Fresh EC was washed three times with tap water to remove salt, epiphytes, and sand, and stored at −20 °C. Frozen samples were lyophilised and homogenised using a grinder before extraction. Phlorotannins were isolated from EC powder as described by Heo et al. (2009) with slight modifications. Briefly, dried EC powder (500 g) was extracted three times with 80% MeOH and then filtered. The filtrate was evaporated at 40 °C to obtain a methanol extract, which was suspended in distilled water and partitioned with ethyl acetate. The ethyl acetate fraction was mixed with Celite, dried, packed into a glass column, and eluted using hexane, methylene chloride, diethyl ether, and methanol, in that order. The diethyl ether fraction was further purified by Sephadex LH-20 column chromatography using a stepwise gradient of chloroform/methanol (2:1 → 0:1).

### 2.3. Spectrophotometric determination of phlorotannin

The total phlorotannin content in the extract was determined according to a modified Folin–Ciocalteu method (Waterman & Mole, 1994), using phloroglucinol as a standard. Samples were diluted, taking into account the detection range of the spectrophotometer (e.g., a 0.005-mL aliquot of soluble phenolic extract was mixed with 0.495 mL of water). A 0.1-mL aliquot of the diluted sample was mixed with 1.0 mL of 1 N Folin–Ciocalteu reagent. The mixture was allowed to stand for 3 min, followed by the addition of 2.0 mL of 20% $Na_2CO_3$. The sample was incubated in the dark at room temperature for 45 min and then clarified by centrifugation at 1600 × *g* for 8 min. The optical density (OD) of the supernatant was measured at 730 nm using a BIO-TEK® Powerwave XS microplate reader (Bio-Tek Instruments, Inc., Winooski, VT, USA). Total phlorotannin content was calculated using the standard curve and is expressed as a percentage.

### 2.4. Fabrication of PCL/phlorotannin micro/nanofibres

As shown in Fig. 1a, the electrospinning process was conducted using an auxiliary electrode to lower the instability of the initial spun jet leaving the apex of the Taylor cone. The polymer solution was placed in a 10-mL glass syringe with a 21 G needle. The feed rate of the solution (1 mL/h) was precisely controlled by a syringe pump system (KDS 230; KD Scientific). The applied electric field was 0.83 kV/cm, and a high-voltage direct current supplier (HVDC, SHV300RD-50K; Convertech) was used to control the applied voltage. A constant needle-to-collector distance of 120 mm and collector rotation speeds of 1.6 (300 rpm) and 6.8 m/s (1300 rpm) were used. The solutions used were pure PCL, PCL with 1 wt% phlorotannin (PCL/Ph-1), PCL with 3 wt% phlorotannin (PCL/Ph-2), and PCL with 5 wt% phlorotannin (PCL/Ph-3).

### 2.5. Characterisation of PCL/phlorotannin fibrous mats

The morphology of the electrospun biocomposites was observed under an optical microscope (BX FM-32; Olympus) connected to a digital camera and under a scanning electron microscope (SEM; Sirion). The mechanical behaviour of the biocomposites was characterised using a microtensile tester (Toptech 2000; Chemilab) in tensile mode. Samples measuring 10 mm × 15 mm were prepared, and the mechanical data were acquired in five independent experiments. All data are presented as mean values with standard deviation (SD). Specimen thickness was measured at five different points under an optical microscope, and the values were averaged. To observe the mechanical behaviour of the biocomposites, samples were prepared parallel to the direction of rotation of a uniaxially aligned fibre mat. The samples were stretched to failure at a stretching speed of 0.5 mm/s at room temperature.

The water contact angles for five independent mats were averaged and are presented as the mean ± SD. Water (10 mL) was placed on the surface of the pure PCL and PCL/Ph mats, and the contact angle was measured under an atmospheric temperature of 26 °C and humidity of 37%. Water absorption was calculated by weighing the mats before and after soaking in distilled water for 30 min. The percentage increase in water absorption was calculated as $(W_{30m} - W_o)/W_o \times 100$, where $W_{30m}$ is the weight of the scaffold after 30 min and $W_o$ is the original weight of the scaffold at time zero.

### 2.6. In vitro cell culture

Fabricated fibrous PCL/Ph mats (10 mm × 10 mm) were sterilised with 70% EtOH and UV light, and then placed in culture medium overnight. MG63 cells (ATCC, Manassas, VA, USA) were used to observe cell behaviour in the mats. The cells were cultured for up to 14 passages in 24-well plates containing Dulbecco's modified Eagle's medium (Hyclone, Logan, UT, USA) supplemented with 10% foetal bovine serum (Hyclone) and 1% penicillin/streptomycin (Hyclone). The cells were collected by trypsin–EDTA treatment, seeded onto the scaffolds at a density of $1 \times 10^5$/specimen, and incubated at 37 °C in an atmosphere of 5% $CO_2$. The medium was changed every second day. To assess cell morphology, after 7 days of culturing, the cell/specimen constructs were fixed in 2.5% glutaraldehyde, dehydrated through a graded ethanol series, coated with gold, and examined under a SEM. Cell growth was determined by the MTT [3-(4,5-dimethylthiazol-2-yl)-2,5-diphenyl tetrazolium bromide] assay (Cell Proliferation

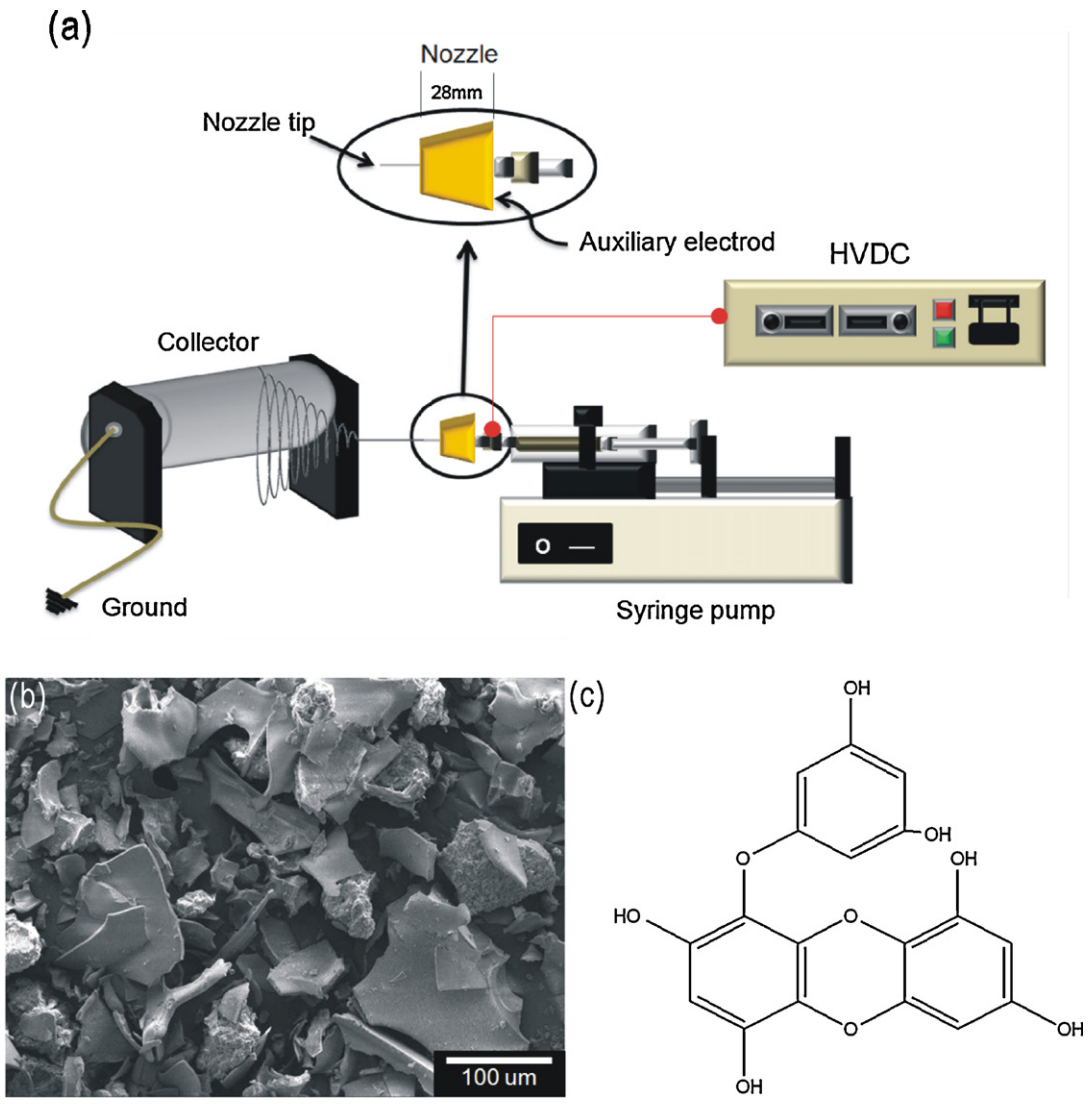


**Fig. 1.** (a) Schematic of the electrospinning process with an auxiliary electrode for fabricating PCL/phlorotannin micro/nanofibres, (b) SEM image of phlorotannin powder, and (c) the chemical structure of phlorotannin.

Kit I; Boehringer Mannheim, Mannheim, Germany). In this assay, mitochondrial dehydrogenases of viable cells cleave the yellow MTT substrate to produce purple formazan crystals. Cells on mats were incubated with MTT (0.5 mg mL$^{-1}$) for 4 h at 37 °C, and the absorbance at 570 nm was measured using a microplate reader (EL800; Bio-Tek Instruments). Five samples were tested during the incubation period, and each test was performed in triplicate.

### 2.7. Alkaline phosphatase activity

ALP, which is a marker of osteoblast activity, was assayed by measuring the release of p-nitrophenol from p-nitrophenyl phosphate (p-NPP). Scaffolds seeded with osteoblast-like cells were rinsed gently with PBS and incubated for 10 min in Tris buffer (10 mM, pH 7.5) containing 0.1% Triton X-100. Then, 100 μL of the lysate was added to the wells of 96-well tissue culture plates containing 100 μL of p-NPP solution, prepared using an alkaline phosphatase kit (Procedure No. ALP-10; Sigma). In the presence of ALP, p-NPP is transformed to p-nitrophenol and inorganic phosphate. ALP activity was determined from the absorbance at 405 nm, using a microplate reader (Spectra III; SLT-Lab Instruments, Salzburg, Austria). ALP activity was normalised to total protein content.

### 2.8. Alizarin Red S staining

Calcium mineralisation was determined by Alizarin Red S staining of MG63 cells in 24-well plates. MG63 cells were cultured in DMEM containing 50 μg mL$^{-1}$ vitamin C and 10 mM β-glycerophosphate. The cells were then washed three times with PBS, fixed in 70% (v/v) cold ethanol (4 °C) for 1 h, and air-dried. The ethanol-fixed specimens were stained with 40 mM Alizarin Red S (pH 4.2) for 1 h and washed three times with purified water. An optical microscope was used to observe the extent of staining.

### 2.9. Total protein content

Total protein content was measured using a bicinchoninic acid (BCA) protein assay (Pierce kit; Thermo Scientific). Cell/scaffold samples were assayed after culturing for 7 and 14 days. Specimens were washed with PBS and lysed with 1 mL of 0.1% Triton X-100. An aliquot of the lysate (25 μL) was added to 200 μL of BCA working reagent, and the mixture was incubated for 30 min at 37 °C. The absorbance at 562 nm was determined using a plate reader, and the total protein concentration was calculated using a standard curve.

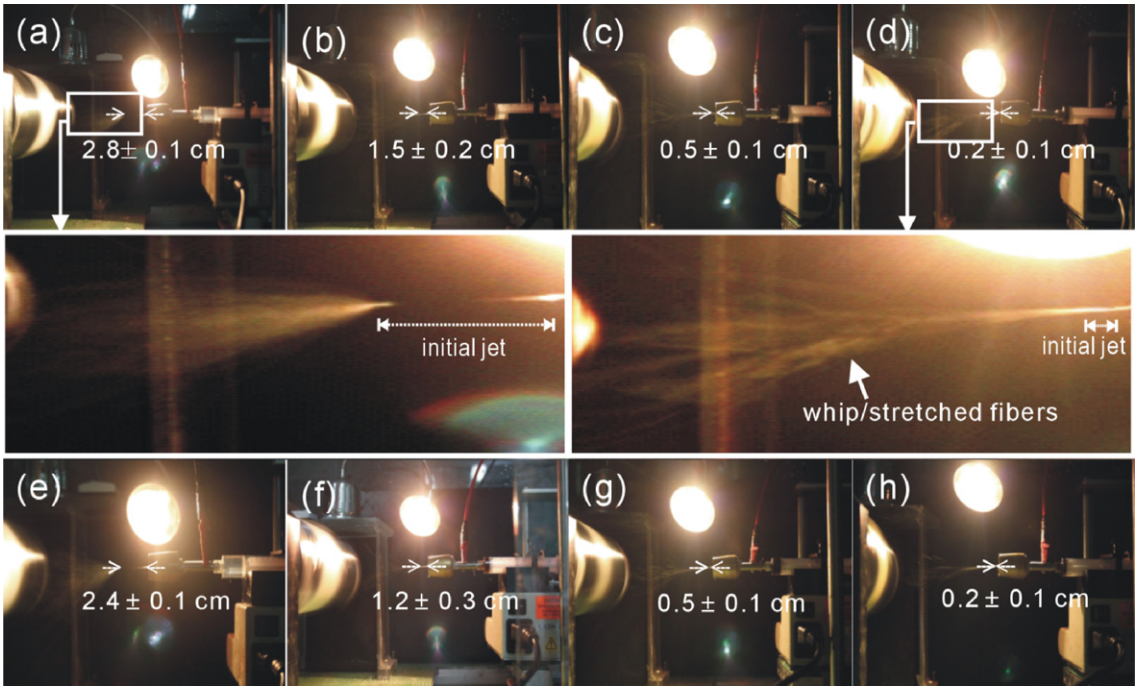


**Fig. 2.** Whipping motion and initial jets for electrospun fibres of (a) pure PCL, (b) PCL/Ph-1, (c) PCL/Ph-2, (d) PCL/Ph-3, (e) pure PCL, (f) PCL/P-1, (g) PCL/P-2, and (h) PCL/P-3. Collector rotation speeds were (a–d) 1.6 m/s and (e–f) 6.8 m/s.

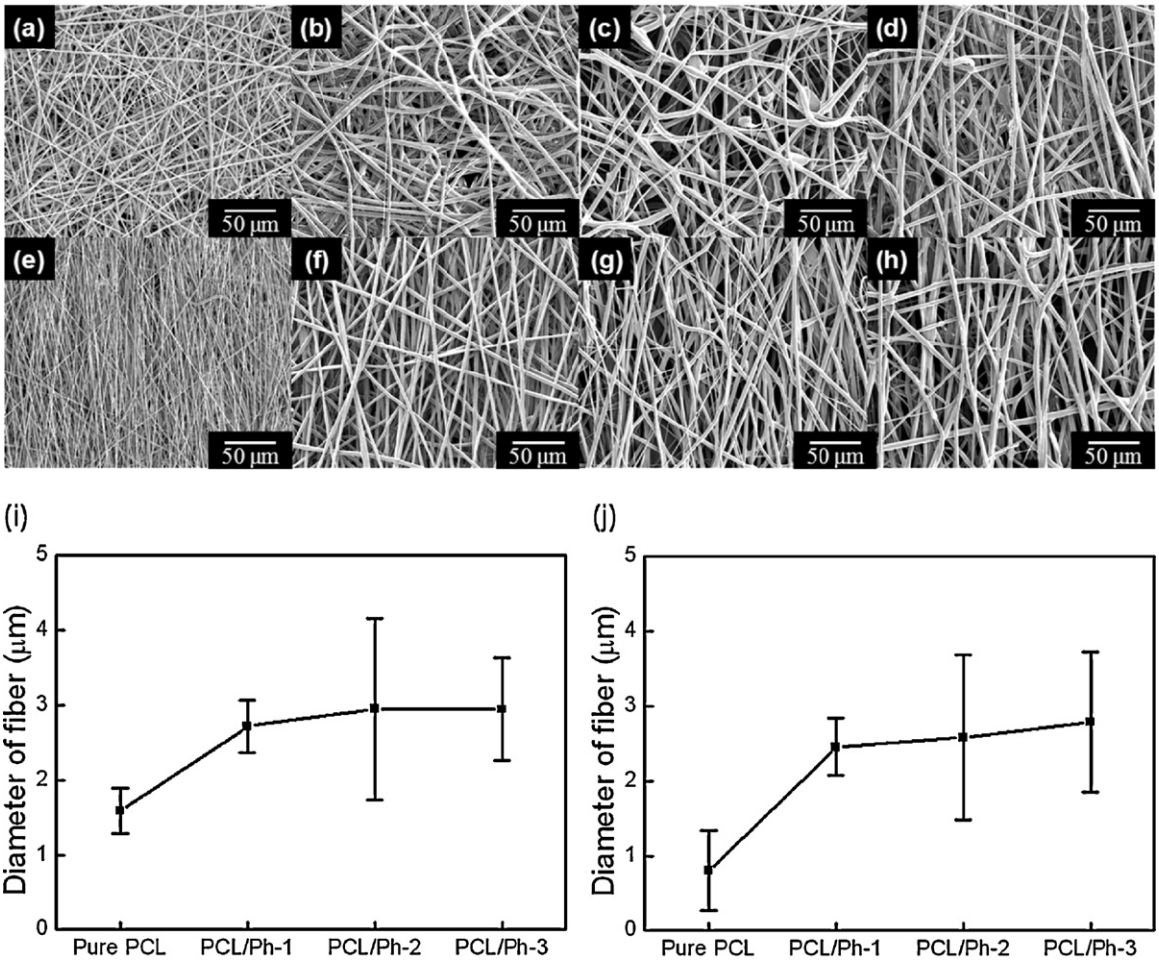


**Fig. 3.** SEM images of micro/nanofibres containing various weight fractions of phlorotannin and fabricated at two different collector rotation speeds (1.6 and 6.8 m/s). At 1.6 m/s: (a) pure PCL, (b) PCL/Ph-1, (c) PCL/Ph-2, and (d) PCL/Ph-3. At 6.8 m/s: (e) pure PCL, (f) PCL/Ph-1, (g) PCL/Ph-2, and (h) PCL/Ph-3. Mean diameters of micro/nanofibres composed of pure PCL and various PCL/Ph mixtures fabricated at collector rotation speeds of (i) 1.6 m/s and (j) 6.8 m/s.

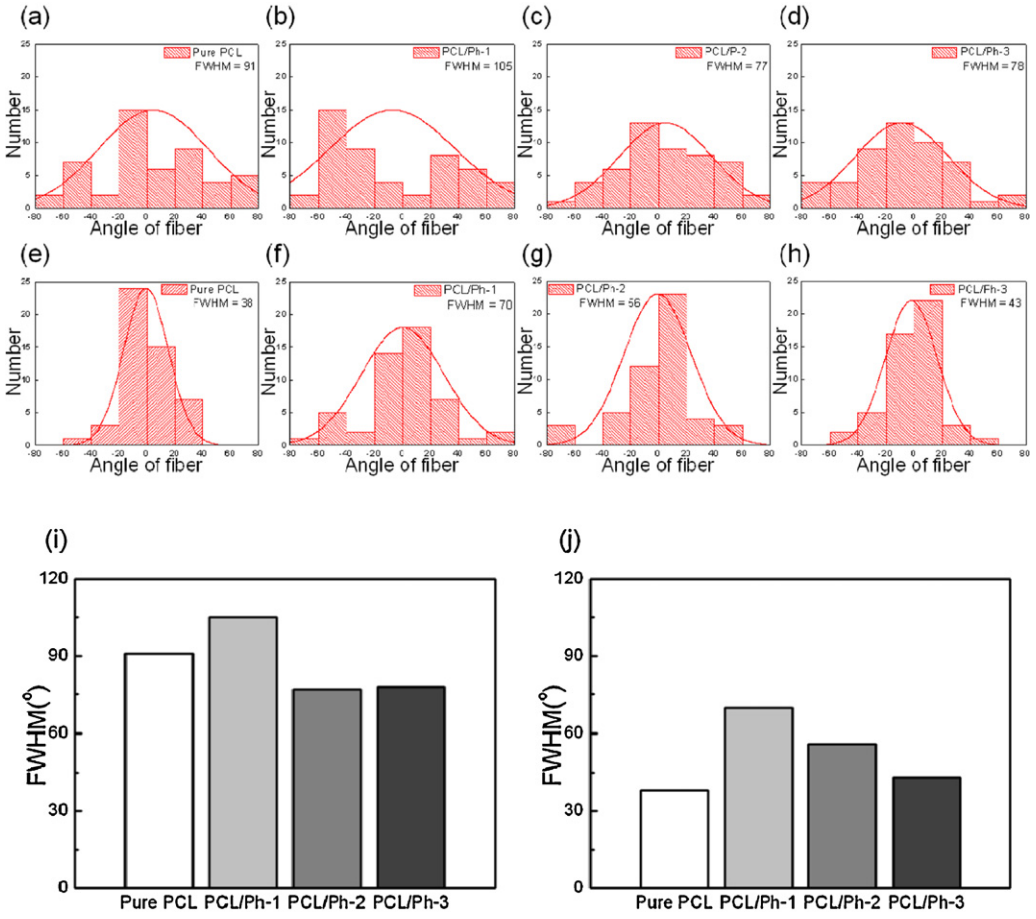


**Fig. 4.** Alignment of fibres composed of pure PCL and PCL with various weight fractions of phlorotannin fabricated at two different collector rotation speeds, (a–d) 1.6 m/s and (e–h) 6.8 m/s. (i and j) The degree of full width at half maximum (FWHM) for fibres composed of pure PCL and PCL with various concentrations of phlorotannin for two different rolling speeds (1.6 m/s and 6.8 m/s), respectively.

### 2.10. Statistical analysis

All data are presented as means ± SD. Statistical analyses consisted of single factor analyses of variance (ANOVA). In all analyses, $P < 0.05$ was taken to indicate statistical significance.

## 3. Results and discussion

### 3.1. Phlorotannin content

Phlorotannin is produced entirely by polymerisation of phloroglucinol, which is a product of the acetate–malonate pathway, also known as the polypeptide pathway. EC extract consisted of 91.08 ± 0.65% phlorotannin on a dry weight basis. Fig. 1b shows a SEM image of phlorotannin powder (Fig. 1b) and the chemical structure of phlorotannin (Fig. 1c).

### 3.2. Electrospinning process for micro/nanofibre formation

Fig. 2a–h shows the general whipping/stretching motion of fibres during the electrospinning process, and the distance of the initial jet between the nozzle tip and the whipping starting point. The distance of the initial jet decreased with an increasing phlorotannin weight fraction. This was attributable to the increased electrical conductivity of the PCL/Ph solutions compared with pure PCL, although the surface tension was increased with increasing phlorotannin weight fraction (Table 1). Because of the high electrical conductivity, positively charged ions in the solution are electrostatically repulsed between fibres, so that the initial jet is shortened.

### 3.3. Morphological analysis of fabricated pure PCL and PCL/Ph micro/nanofibres

Fig. 3 (panels a–h) shows SEM images of electrospun micro/nanofibres containing pure PCL, PCL/Ph-1 (1 wt%), PCL/Ph-2 (3 wt%), or PCL/Ph-3 (5 wt%) that were generated using two different collector rotation speeds, 1.6 m/s (panels a–d) and 6.8 m/s (panels e–h). The alignment of the electrospun fibres was improved at the higher rotation speed.

As shown in Fig. 3i and j, the average diameter of the micro/nanofibres increased with an increasing phlorotannin weight fraction. This phenomenon can be explained by the simplified Fridrikh equation (Fridrikh, Yu, Brenner, & Rutledge, 2003),

$$d_f \propto (\gamma)^{1/3} \left( \frac{1}{\ln(\kappa)^{1/3}} \right),$$

**Table 1**
Electrical conductivity and surface tension of pure PCL and PCL/Ph solutions.

| Parameter | Pure PCL | PCL/Ph-1 | PCL/Ph-2 | PCL/Ph-3 |
|---|---|---|---|---|
| Conductivity (μS/cm) | 1.3 ± 0.3 | 48.8 ± 0.3 | 62.6 ± 0.4 | 69.9 ± 0.5 |
| Surface tension (N/m) | 0.021 | 0.028 | 0.042 | 0.046 |

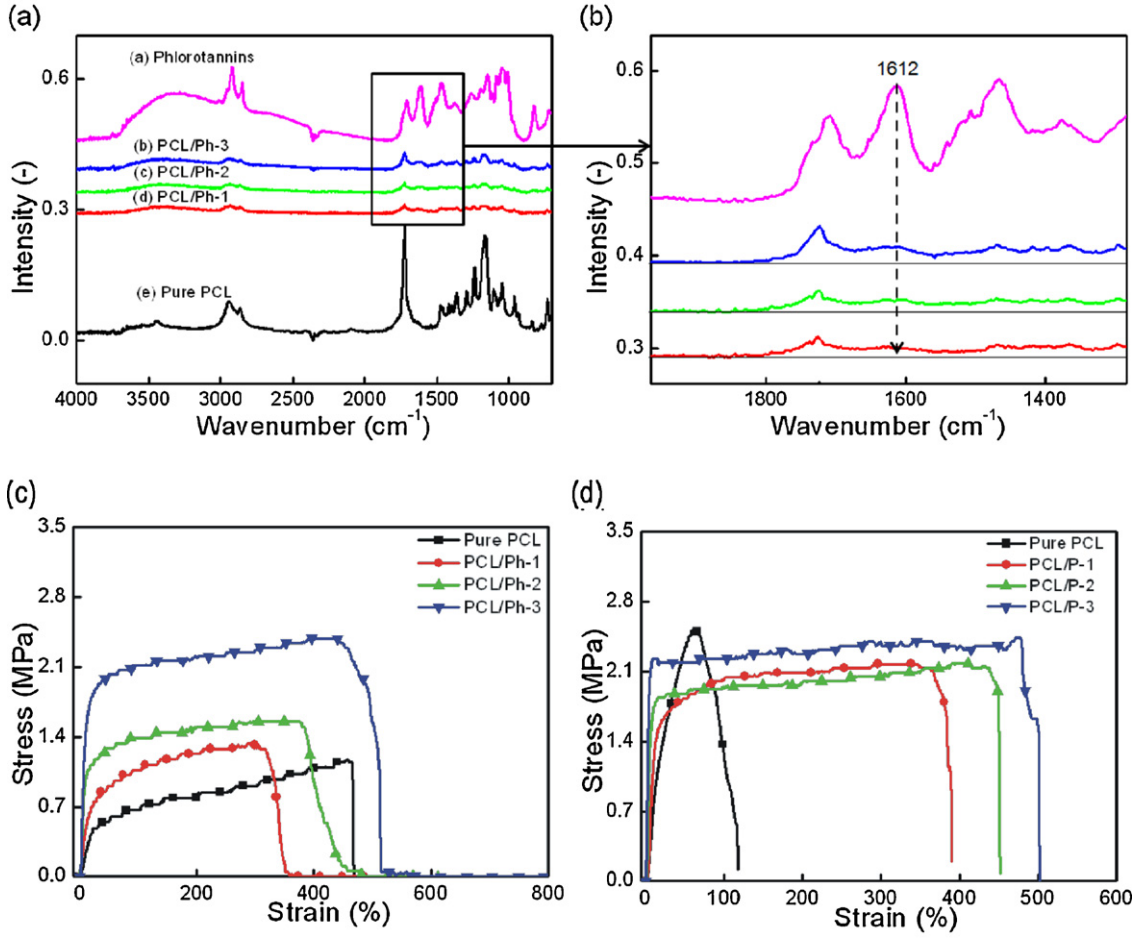


**Fig. 5.** (a) FT-IR of mats composed of pure PCL, pure phlorotannins, and PCL/Ph, (b) magnification of the boxed area of the graph in (a). Stress–strain curves for mats composed of pure PCL and PCL/Ph fabricated at collector rotation speeds of (c) 1.6 m/s and (d) 6.8 m/s.

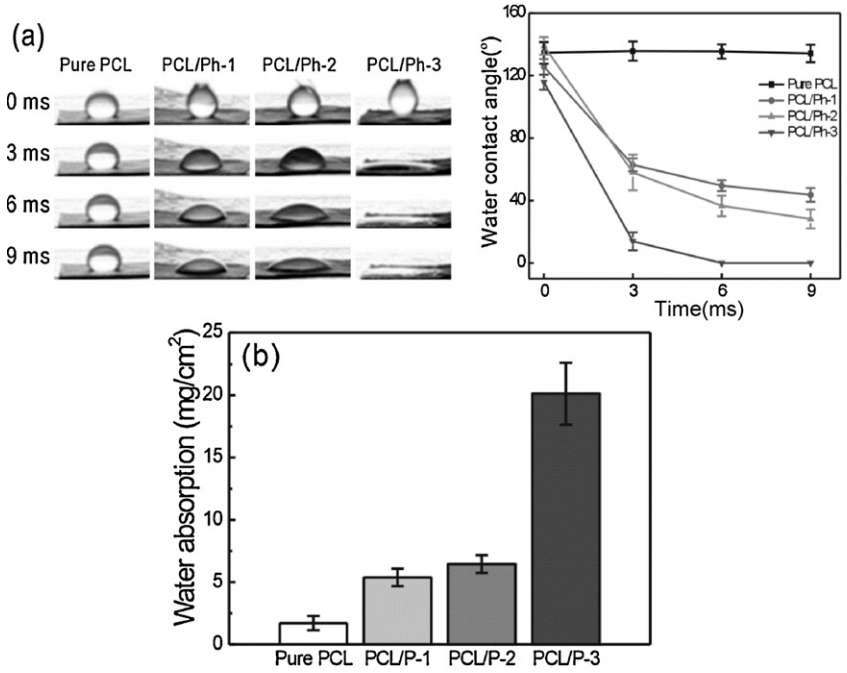


**Fig. 6.** (a) Water contact angle measurements and (b) water absorption of mats composed of pure PCL and PCL/Ph fabricated using a collector rotation speed of 1.6 m/s ($n = 5$).

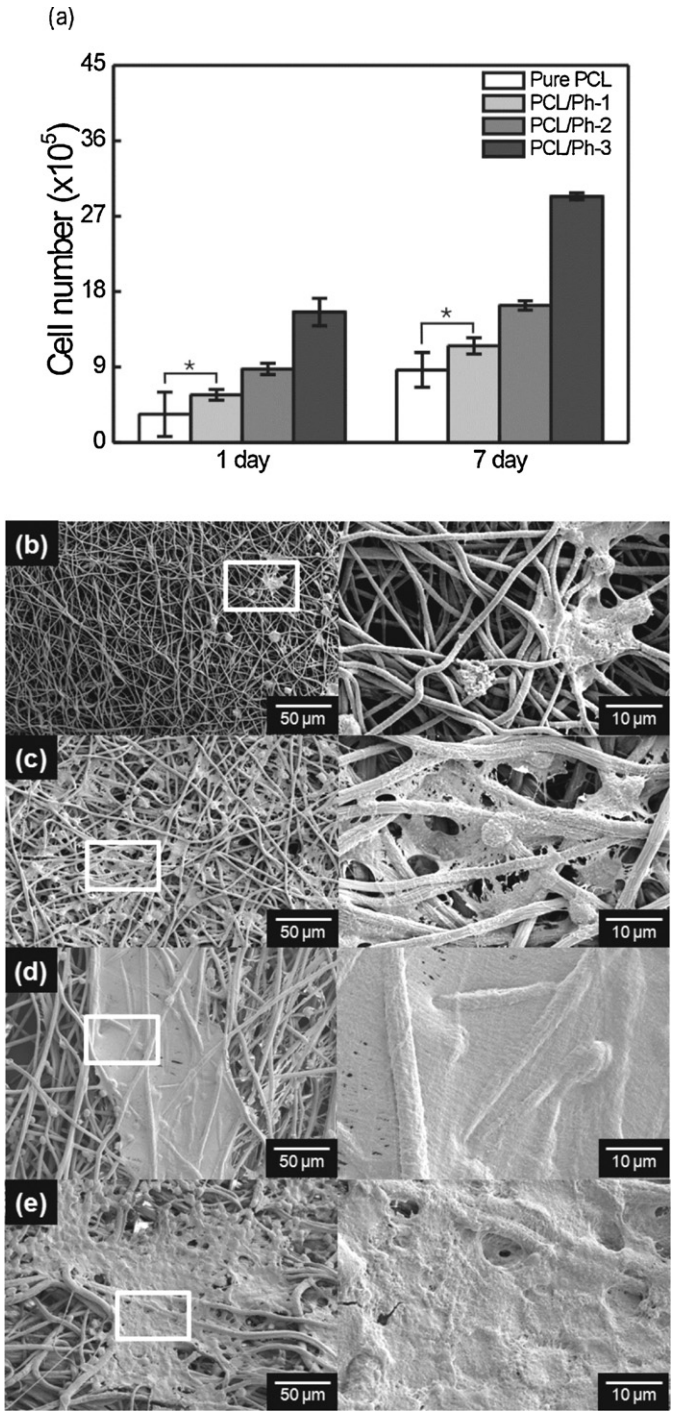


**Fig. 7.** Cell viability of MG63 cells cultured on mats composed of pure PCL and PCL/Ph for 1 and 7 days. SEM micrographs of MG63 cells cultured on mats composed of (b) pure PCL, (c) PCL/Ph-1, (d) PCL/Ph-2, and (e) PCL/Ph-3 for 7 days.

where $d_f$ is the calculated fibre diameter, $\gamma$ is surface tension, and $\kappa$ is the length of the initial jet. Although a solution with higher electrical conductivity generally results in a reduced micro/nanofibre final diameter, the addition of phlorotannin in our study also produced an increase in surface tension. For this reason, as predicted by the theoretical estimation, the diameter of PCL/Ph micro/nanofibres was about 32% greater than that of pure PCL micro/nanofibres.

The alignment of electrospun micro/nanofibres to control cell alignment is vital in tissue regeneration because establishing the orientation of cells as in the native tissue may be critical for tissue function (Teo & Ramakrishna, 2006). We measured the alignment of micro/nanofibres in PCL/Ph electrospun mats using SEM images. Fig. 4 shows the alignments of fibres generated at 1.6 m/s (panels a–d) and 6.8 m/s (panels e–h). Fibre alignment is also described as the degree of full width at half maximum (FWHM) for two different collector speeds for 1.6 m/s (Fig. 4i) and 6.8 m/s (Fig. 4j). Fibre alignment increased with an increase in the collector rotation speed. The FWHM was highest for PCL/Ph-1, possibly because a small quantity of phlorotannin particles distributed irregularly on the collector disturbed the uniform alignment of the fibres. The alignment of PCL/Ph fibres was improved when the phlorotannin weight fraction was increased, as this lowered the sporadic distribution of high concentrations of positively charged phlorotannin in the fibres. This theoretical explanation is validated by the FWHM data (Fig. 4i and j).

### 3.4. FT-IR analysis of PCL/Ph mats

Fig. 5a and b shows the FT-IR results for mats composed of pure PCL, pure phlorotannin, and PCL/Ph containing different phlorotannin concentrations. In the phlorotannin spectrum, the bands at 1612, 1482, and 1375 $cm^{-1}$ are attributable to the aromatic ring structure of phlorotannin (Yan, Li, Zhou, & Fan, 1996). In addition, the broad IR band at 1267 $cm^{-1}$ is due to the aromatic ether stretch. The majority of the IR bands of phlorotannin and PCL were coupled; however, the band at 1612 $cm^{-1}$ differed slightly between phlorotannin and PCL. Thus, to quantify the level of phlorotannin in mats, we compared the 1612 $cm^{-1}$ regions of the spectra. The peak at 1612 $cm^{-1}$ increased gradually with increasing phlorotannin weight fraction (Fig. 5b). Based on these FT-IR results, we suggest that the phlorotannin weight fractions of the composites correlated well with the designed phlorotannin levels in the PCL/Ph fibres and that the chemical structure of phlorotannin was not completely changed upon its incorporation into the electrospun fibres.

### 3.5. Mechanical properties

To observe the orthotropic mechanical behaviour of electrospun PCL/Ph fibrous mats, specimens (15 mm × 10 mm) of the fabricated electrospun mats were analysed using a tensile test performed at room temperature. Stress–strain curves were measured, with the samples parallel to the rotating collector, for mats composed of pure PCL and PCL/Ph containing different phlorotannin at weight fractions fabricated at collector speeds of 1.6 (Fig. 5c) and 6.8 m/s (Fig. 5d). In general, the elastic modulus was closely related to the fibre alignment in the electrospun mat. As the rotation speed of the collector increased, the mechanical properties of both pure PCL and the PCL/Ph mats improved. In particular, Young's modulus was higher for all PCL/Ph mats compared with the pure PCL mat. This result could be analysed using the modified Halpin–Tsai equation. However, this equation requires that the modulus of pure phlorotannin be known, and this is very difficult to measure because of the brittle nature of phlorotannin. Thus, we were unable to analyse the mechanical data using this equation. Nevertheless, the increased modulus may be explained as follows. During the stretching of the mats, the PCL matrix was the first to deform, while the phlorotannin in the fibres acted as a reinforcing bridge and increased the resistance to deformation. Table 2 shows the detailed tensile properties of the samples parallel to the rotation direction.

### 3.6. Water contact angle and water absorption of PCL/phlorotannin mats

The hydrophilicity of a material contributes significantly to initial cell attachment, cell proliferation, and cell migration (Boyan, Hummert, Dean, & Schwartz, 1996; Howlett, Evans, Walsh, Johnson,

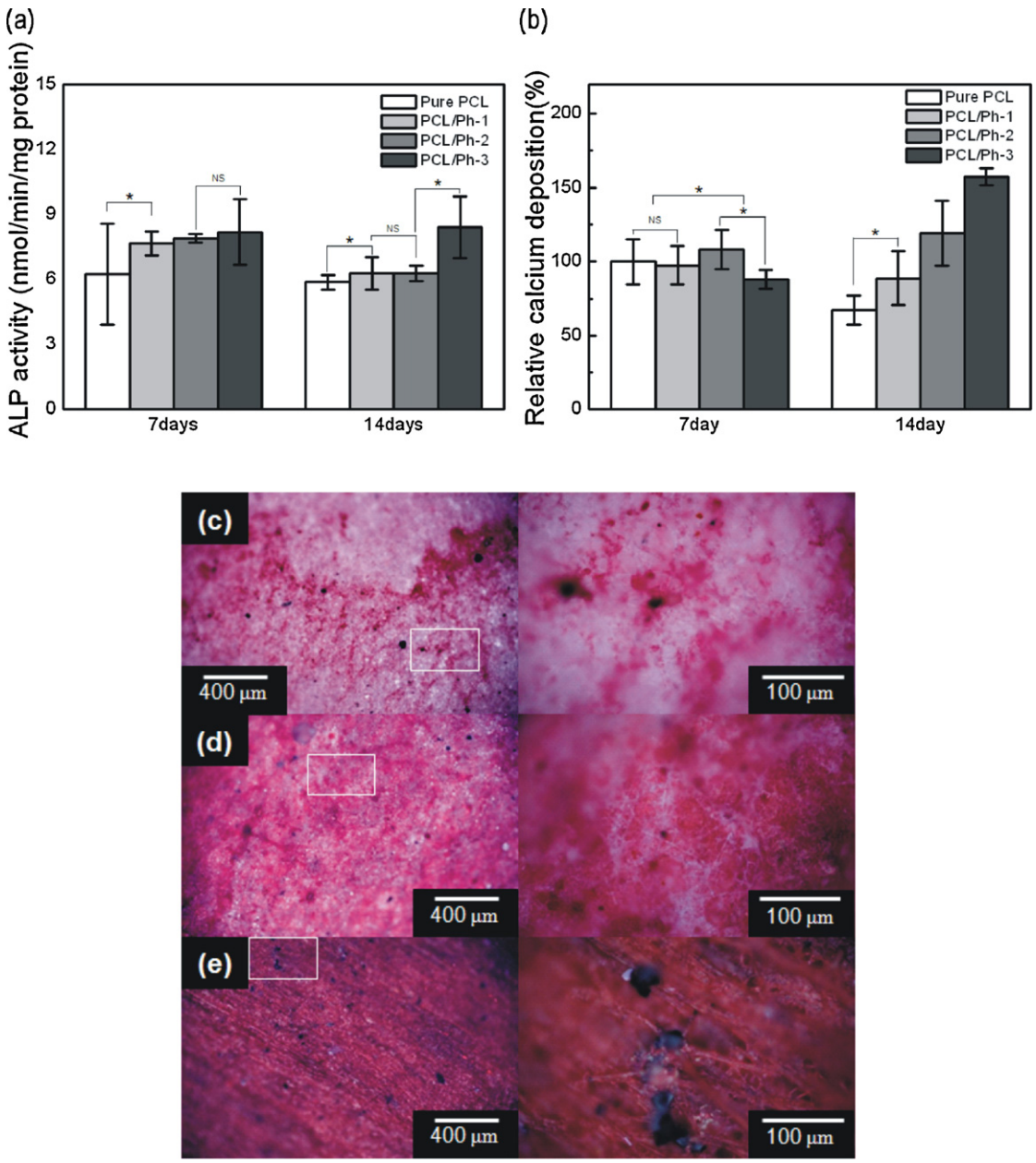


**Fig. 8.** (a) Alkaline phosphatase activity of MG63 cells cultured on mats composed of pure PCL and PCL/Ph for 7 and 14 days. (b) Relative calcium deposition by MG63 cells cultured on pure PCL and PCL/Ph mats for 7 and 14 days. Alizarin Red S staining of mats composed of (c) pure PCL, (d) PCL/Ph-1, and (e) PCL/Ph-3 after 14 days of cell culture.

**Table 2**
Mechanical properties of electrospun mats composed of pure PCL and PCL/Ph.

| Sample type | | Pure PCL | | | PCL/Ph-1 | | |
|---|---|---|---|---|---|---|---|
| Collector speed | Stretching velocity (mm/s) | Young's modulus (MPa) | Max. tensile strength (MPa) | Strain at break (%) | Young's modulus (MPa) | Max. tensile strength (MPa) | Strain at break (%) |
| 1.6 m/s | 0.5 | 2.9 ± 0.1 | 1.2 | 464.1 ± 0.2 | 5.6 ± 0.1 | 1.3 | 316.3 ± 0.2 |
| 6.8 m/s | 0.5 | 9.2 ± 0.6 | 2.5 | 66.0 ± 1.4 | 15.9 ± 1.5 | 2.2 | 365.4 ± 0.1 |
| Sample type | | PCL/Ph-2 | | | PCL/Ph-3 | | |
| Collector speed | Stretching velocity (mm/s) | Young's modulus (MPa) | Max. tensile strength (MPa) | Strain at break (%) | Young's modulus (MPa) | Max. tensile strength (MPa) | Strain at break (%) |
| 1.6 m/s | 0.5 | 12.9 ± 6.3 | 1.6 | 376.3 ± 0.2 | 27.3 ± 3.5 | 2.4 | 438.8 ± 1.5 |
| 6.8 m/s | 0.5 | 37.1 ± 7.9 | 2.2 | 437.5 ± 0.5 | 57.8 ± 6.6 | 2.5 | 477.5 ± 0.2 |

**Table 3**
Total protein content of MG63 cells extracted from mats composed of pure PCL and PCL/Ph fabricated at 1.6 m/s.

| Culture time | Pure PCL | PCL/Ph-1 | PCL/Ph-2 | PCL/Ph-3 |
|---|---|---|---|---|
| 7 days | 16.54 ± 4.05 mg | 24.63 ± 9.65 mg | 27.65 ± 8.03 mg | 45.19 ± 1.01 mg |
| 14 days | 36.86 ± 12.80 mg | 35.27 ± 5.95 mg | 35.43 ± 0.67 mg | 42.33 ± 9.76 mg |

& Steele, 1994). To assess the effect of phlorotannin on the hydrophilicity of the fibres, the water contact angle (WCA) and water absorption ability were measured and compared with those of pure PCL fibres. In general, given that phlorotannin is highly hydrophilic, the PCL/Ph mats would be expected to exhibit higher hydrophilicity and water absorption compared with the pure PCL mat. This hypothesis was confirmed by the measured WCAs (Fig. 6a) and water absorption (Fig. 6b). WCA was dramatically decreased and water absorption was increased with increasing phlorotannin content. In particular, PCL/Ph-3 showed an abrupt increase in hydrophilicity and water absorption ability. Thus, the advantage of PCL/Ph-3 fibres for cellular behaviour is likely to be greater than that of fibres with the other phlorotannin percentages.

### 3.7. *In vitro* cell viability

To evaluate the effects of phlorotannin-containing fibres on cell viability, MG63 osteoblast-like cells were cultured with mats composed of pure PCL and PCL/Ph fabricated using a collector speed of 1.6 m/s. The micro/nanoscale of a fibrous structure generally promotes cell growth because of its high surface-to-volume ratio. As shown in Fig. 7a, the pure PCL mat exhibited the lowest cell viability at 1 day, and cell viability gradually increased on PCL/Ph mats with increasing phlorotannin content. In particular, PCL/Ph-3 supported the greatest cell viability. We believe that this was attributable to the high hydrophilicity and water absorption of PCL/Ph-3 mats, as well as the biological assistance provided by phlorotannin.

SEM micrographs (Fig. 7b–e) revealed the morphological features of MG63 cells cultured for 7 days on mats of pure PCL and PCL/Ph-1, -2, and -3 fibres, respectively. Proliferating MG63 cells were adhered sporadically on a small region of the pure PCL mat, whereas most of the PCL/Ph-3 mat was covered with cells, indicating that phlorotannin-containing mats possessed a high affinity for cells compared with the pure PCL mat. These results are consistent with the cell viability data.

ALP activity is an early osteoblastic differentiation marker and is produced by cells showing a mineralised extracellular matrix (Gotoh, Hiraiwa, & Narajama, 1990). Fig. 8a shows the relative ALP activity, normalised to the total protein content (Table 3), of cells cultured with the mats for 7 and 14 days. Although the relative ALP activity did not increase with time, the ALP activity associated with the PCL/Ph-3 mat was higher than that associated with the other mats at 14 days.

To evaluate calcium mineralisation, Alizarin Red S staining was performed to assess the calcium concentrations of the pure PCL and PCL/Ph mats after 14 days of cell culture (Fig. 8b). Mineralisation was significantly higher for the PCL/Ph mats compared with the pure PCL mats at day 14 (Fig. 8b), suggesting that the addition of phlorotannin to the fibres significantly increased mineralisation. In the optical images (Fig. 8c–e), the highly intense (almost black) Alizarin Red S staining indicates higher calcium concentrations. The biological activities (cell viability, ALP activity, total protein content, and calcium mineralisation) of electrospun PCL mats demonstrate that the inclusion of phlorotannin enhances cell viability and mineralisation of these fibres as a substrate for bone tissue regeneration.

## 4. Conclusion

Using an electrospinning process, we fabricated PCL/Ph micro/nanofibrous mats with various phlorotannin content (1, 3, and 5 wt%). Compared with the pure PCL mats, the mats containing 5% phlorotannin (PCL/Ph-3 mats) exhibited marked hydrophilicity, greater water absorption (9-fold), and a larger Young's modulus (9-fold). With regard to biological activities, PCL/Ph-3 mats also showed higher cell viability, higher total protein content, increased ALP activity, and greater calcium mineralisation. These data suggest that PCL/Ph electrospun mats represent a potential biomaterial for bone tissue regeneration.

## References


Ahn, M. J., Yoon, K. D., Min, S. Y., Lee, J. S., Kim, J. H., Kim, T. G., et al. (2004). Inhibition of HIV-1 reverse transcriptase and protease by phlorotannins from the brown alga *Ecklonia cava*. *Biological & Pharmaceutical Bulletin*, *27*, 544–547.

Bergshoef, M. M., & Vancso, G. J. (1999). Transparent nanocomposites with ultrathin, electrospun nylon-4,6 fiber reinforcement. *Advanced Materials*, *11*, 1362–1365.

Boyan, B. D., Hummert, T. W., Dean, D. D., & Schwartz, Z. (1996). Role of material surfaces in regulating bone and cartilage cell response. *Biomaterials*, *17*, 137–146.

Chen, C. Y., & Chou, H. N. (2002). Screening of red algae filaments as a potential alternative source of eicosapentaenoic acid. *Journal of Marine Biotechnology*, *4*, 189–192.

Cho, E. K., & Choi, Y. J. (2010). Physiological activities of hot water extracts from *Ecklonia cava* Kjellman. *Journal of Life Science*, *20*, 1675–1682.

Doshi, J., & Reneker, D. H. (1995). Electrospinning process and applications of electrospun fibers. *Journal of Electrostatics*, *35*, 151–160.

Fong, H., Chun, I., & Reneker, D. H. (1999). Beaded nanofibers formed during electrospinning. *Polymer*, *40*, 4585–4592.

Formhals, A. (1934). *Process and apparatus for preparing artificial threads*. United States Patent 1,975,504.

Fridrikh, V., Yu, J. H., Brenner, M. P., & Rutledge, G. C. (2003). Controlling the fiber diameter during electrospinning. *Physical Review Letters*, *90*, 144502.

Frlich, I., & Riederer, P. (1995). Free radical mechanisms in dementia of Alzheimer type and the potential for antioxidant treatment. *Drug Research*, *45*, 443–449.

Gotoh, Y., Hiraiwa, K., & Narajama, M. (1990). In vitro mineralization of osteoblastic cells derived from human bone. *Journal of Bone and Mineral Research*, *8*, 239–250.

Greiner, A., & Wendorff, J. H. (2007). Electrospinning, fascinating method for the preparation of ultrathin fibers. *Angewandte Chemie International Edition*, *46*, 5670–5703.

Heo, S. J., Ko, S.-C., Cha, S.-H., Kang, D.-H., Park, H.-S., Choi, Y.-U., et al. (2009). Effect of phlorotannins isolated from *Ecklonia cava* on melanogenesis and their protective effect against photo-oxidative stress induced by UV-B radiation. *Toxicology In Vitro*, *23*, 1123–1130.

Hirano, Y., & Mooney, D. J. (2004). Peptide and protein presenting materials for tissue engineering. *Advanced Materials*, *16*, 17–25.

Hollister, S. J. (2005). Porous scaffold design for tissue engineering. *Nature Materials*, *4*, 518–524.

Hong, S., & Kim, G. H. (2010). Electrospun polycaprolactone/silk fibroin/small intestine submucosa composites for biomedical applications. *Macromolecular Materials and Engineering*, *295*, 529–534.

Howlett, C. R., Evans, M. D. M., Walsh, W. R., Johnson, G., & Steele, J. G. (1994). Mechanism of initial attachment of cells derived from human bone to commonly used prosthetic materials during cell culture. *Biomaterials*, *3*, 213–222.

Huang, Z. M., Zhang, Y. Z., Kotaki, M., & Ramakrishna, S. (2003). A review on polymer nanofibers by electrospinning and their applications in nanocomposites. *Composite Science and Technology*, *63*, 2223–2253.

Jimenez-Escring, A., & Goni Cambrodon, I. (1999). Nutritional evaluation and physiological effects of edible seaweeds. *Archivos Latinoamericanos de Nutrición*, *49*, 114–120.

Kang, K., Park, Y., Hwang, H. J., Kim, S. H., Lee, J. G., & Shin, H. C. (2003). Antioxidative properties of brown algae polyphenolics and their perspectives as chemopreventive agents against vascular risk factors. *Archives of Pharmacal Research*, *26*, 286–293.

Khademhosseini, A., Langer, R., Borenstein, J., & Vacanti, J. P. (2006). Microscale technologies for tissue engineering and biology. *Proceedings of the National Academy of Sciences of the United States of America*, *103*, 2480–2487.

Kim, G. H., & Kim, W. D. (2006). Nanofiber spraying method using a supplementary electrode. *Applied Physics Letters*, *89*, 013111.

Kumbar, S. G., James, R., Nukavarapu, S. P., & Laurencin, C. T. (2008). Electrospun nanofiber scaffolds: Engineering soft tissues. *Biomedical Materials*, *3*, 034002 (15 pp.).

Luo, C. J., Stride, E., Stoyanov, S., Pelan, E., & Edirisinghe, M. (2011). Electrospinning short polymer micro-fibres with average aspect ratios in the range of 10–200. *Journal of Polymer Research*, *18*, 2515–2522.

Ma, P. X. (2004). Scaffolds for tissue fabrication. *Materials Today*, *7*, 30–40.

Nagayama, K., Iwamura, Y., Shibata, T., Hirayama, I., & Nakamura, T. (2002). Bactericidal activity of phlorotannins from the brown alga *Ecklonia kurome*. *Journal of Antimicrobial Chemotherapy*, *50*, 889–893.

Okai, Y., Higashi-Okai, K., Ishizaka, S., Ohtani, K., Matsui-Yuasa, I., & Yamashita, U. (1998). Possible immunodulating activities in an extract of edible brown alga, *Hijikia fusiforme* (Hijiki). *Journal of the Science of Food and Agriculture*, *76*, 56–62.

Ryu, B. M., Li, Y., Qian, Z.-J., Kim, M.-M., & Kim, S.-K. (2009). Differentiation of human osteosarcoma cells by isolated phlorotannins is subtly linked to COX-2, iNOS, MMPs, and MAPK signaling: Implication for chronic articular disease. *Chemico-Biological Interactions*, *179*, 192–201.

Taylor, G. I. (1964). Disintegration of water drops in an electric field. *Proceedings of the Royal Society of London*, *A280*, 383–397.

Teo, W. E., & Ramakrishna, S. (2006). A review on electrospinning design and nanofiber assemblies. *Nanotechnology*, *17*, R89–R106.

Waterman, P. G., & Mole, S. (Eds.). (1994). *Analysis of phenolic plant metabolites*. Oxford/Boston: Blackwell Scientific.

Yan, X. J., Li, X. C., Zhou, C. X., & Fan, X. (1996). Prevention of fish oil rancidity by phlorotannins from *Sargassum kjellmanianum*. *Journal of Applied Psychology*, *8*, 201–203.